Supplementary Information for

Local Magnetic Moment and Adsorption Energetics as Intrinsic Activity Indicators for Bimetallic 2D π-d Conjugated BHT Frameworks in Oxygen Evolution Electrocatalysis

Kuan-Lun Chen[a], Jing-Yan Wu[a], Yu-Ting Tai[a], Yu-Cheng Kuo[b], Chun-Kai Yeh[a], Ken Sakaushi[*c], Hong-Kang Tian[*abde]

[a] Department of Chemical Engineering, National Cheng Kung University, Tainan 701, Taiwan.

[b] Program on Smart and Sustainable Manufacturing, Academy of Innovative Semiconductor and Sustainable Manufacturing, National Cheng Kung University, Tainan 701, Taiwan.

[c] Research Center for Energy and Environmental Materials, National Institute for Materials Science, Tsukuba, Ibaraki 305-0044, Japan

[d] Center for Resilience and Intelligence on Sustainable Energy Research (RiSER), National Cheng Kung University, Tainan 701, Taiwan

[e] Sustainable Electrochemical Energy Development (SEED) Center, National Taiwan University of Science and Technology, Taipei 106, Taiwan

*E-mail: hktian@gs.ncku.edu.tw (Hong-Kang Tian)

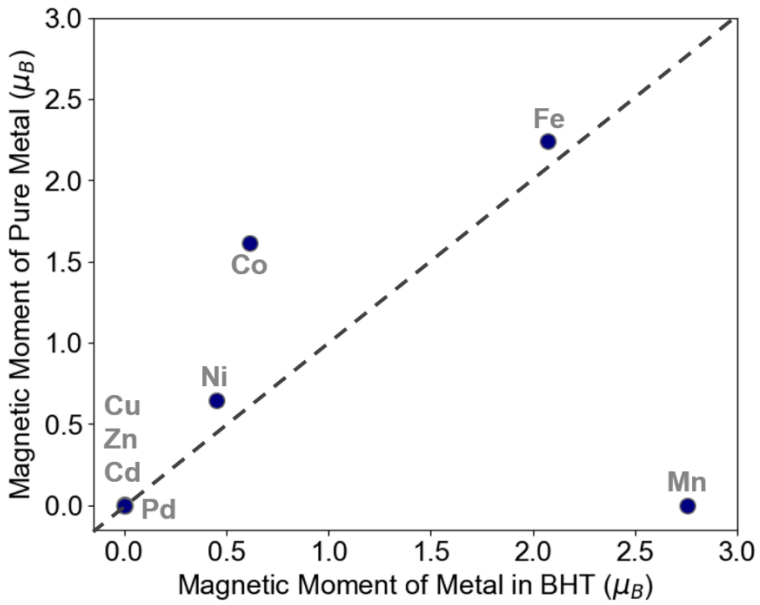

Fig. S1. Comparison between the magnetic moments of pure bulk metals and those of the corresponding metal centers in the BHT-based metal–organic framework. The dashed line indicates the y=x reference, corresponding to no change in magnetic moment after incorporation into the BHT framework.

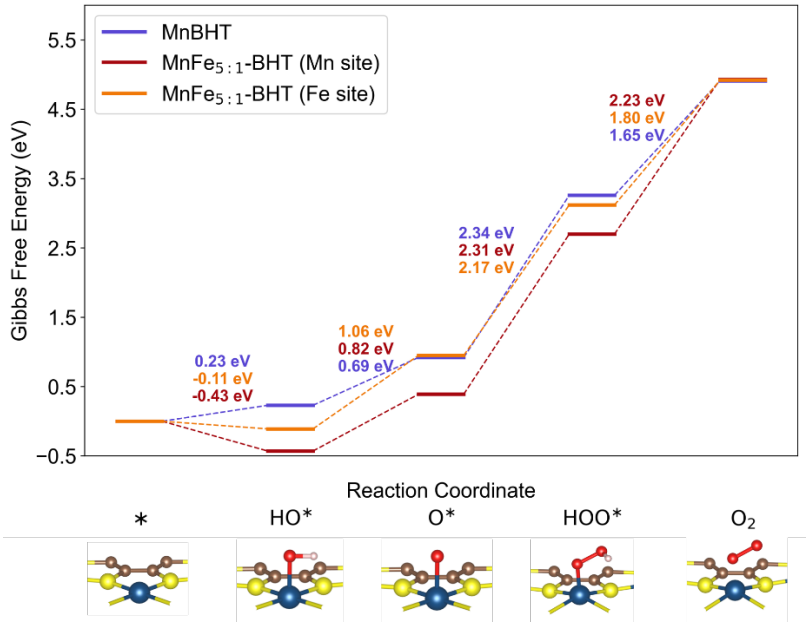

Fig. S2. Computational Hydrogen Electrode (CHE)-level Gibbs free energy profiles (neglecting solvation and applied-potential corrections) for qualitative mechanistic comparison. The energy landscape compares the reaction pathways on the Mn-BHT, $MnFe_{5:1}$-BHT Mn site, and $MnFe_{5:1}$-BHT Fe site. The profiles delineate the four intermediate steps of the electrochemical process. The inserted numerical values represent the specific change in Gibbs free energy between consecutive elementary steps.

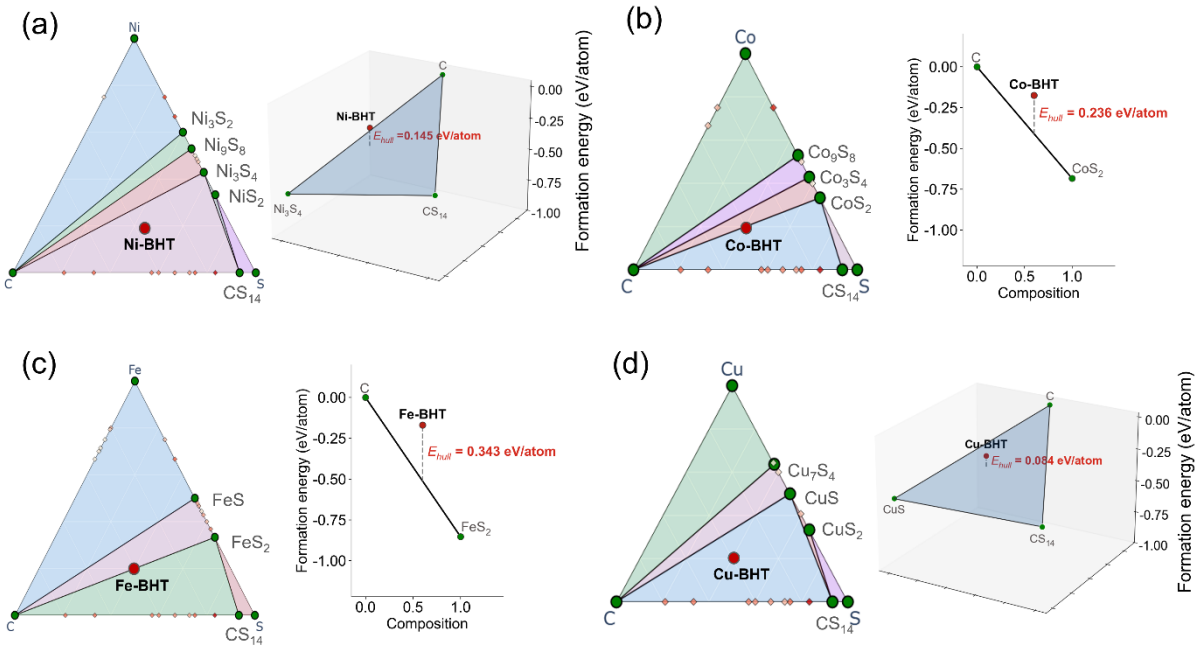

Fig. S3. Thermodynamic stability analysis of TM-BHT monolayers. Phase diagrams and convex hull plots for (a) Ni-BHT, (b) Co-BHT, (c) Fe-BHT, (d) Cu-BHT. The red dots represent the TM-BHT structures, and the calculated $\boldsymbol{E_{hull}}$ values are indicated in red text.

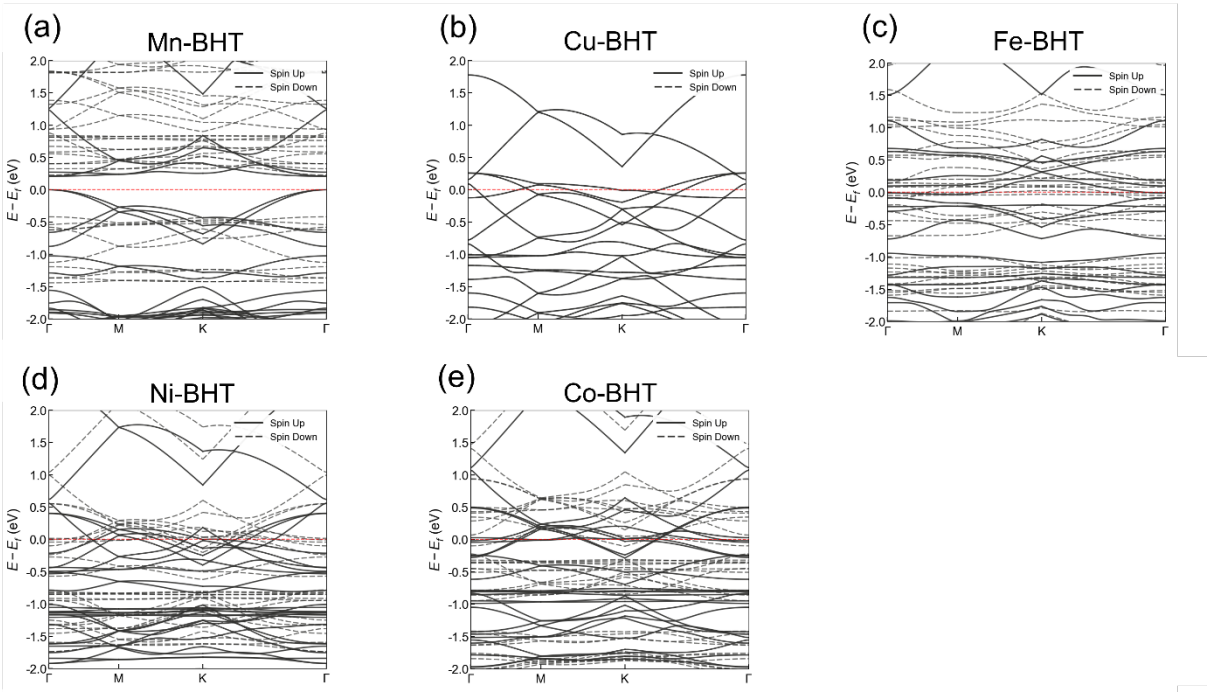

Fig. S4. Band structures of TM-BHT monolayers. Calculated spin-polarized band structures for (a) Mn-BHT, (b) Cu-BHT, (c) Fe-BHT, (d) Ni-BHT, (e) Co-BHT along the high-symmetry path **Γ**-M-K-**Γ**. Solid and dashed lines represent the spin-up and spin-down channels, respectively.

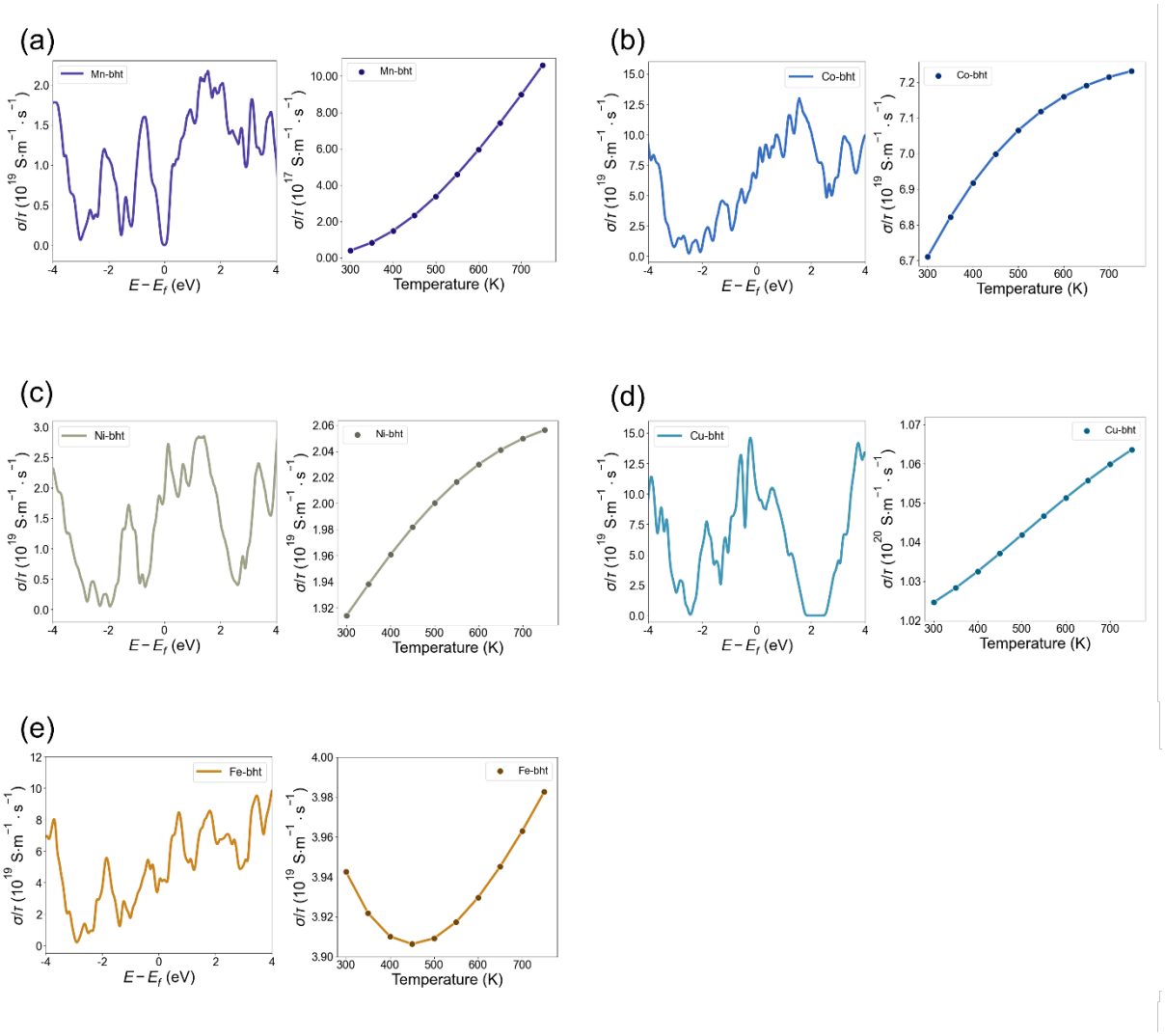

Fig. S5. Electronic transport properties of TM-BHT monolayers. Calculated electrical conductivity scaled by relaxation time ($\boldsymbol{\sigma}/\boldsymbol{\tau}$) as a function of (left) chemical potential relative to the Fermi level at 300 K, and (right) temperature for (a) Mn-BHT, (b) Co-BHT, (c) Ni-BHT, (d) Cu-BHT, (e) Fe-BHT.